Fluoride 2019 Dec 6. www.fluorideresearch.online/epub/files/064.pdf [Epub ahead of print]

PURIFICATION OF SIMULATED FLUORIDE-CONTAMINATED WATER USING SILVER NANOPARTICLES SYNTHESIZED BY *XANTHIUM STUMARIUM* AS A BIO-TEMPLATE

Mudassar Iqbal,[a,*] Muhammad Suleman,[a] Saleem Ullah,[a] Hamida Bibi,[b] Hassan Wahab,[c]
Zafar Iqbal,[a] Khadim Muhammad Dawar,[b] Said Wahab,[d] Muhammad Nauman Ahmad[a]

Peshawar, Pakistan

ABSTRACT: A high concentration of fluoride in water can cause various problems for animals and plants. The aim of this research was to utilize nanotechnology for the treatment of fluoride-contaminated water. For this purpose silver nanoparticles ($AgNP_{(Xs)}$) were synthesised using an aqueous extract of *Xanthium stumarium*as as both a reducing and a stabilizing agent. The synthesised $AgNP_{(Xs)}$ showed Surface Plasmon Resonance at λ 427 nm. Electron microscopy confirmed the particles were evenly distributed rod shaped particles with a size of 28 nm. The infrared spectroscopy confirmed that reactive functional groups could be attached to the $AgNP_{(Xs)}$. Different concentrations of fluoride-contaminated water samples (simulated) were treated with $AgNP_{(Xs)}$, the adsorption of fluoride was measured through UV-Vis spectroscopy, and the fluoride concentration was measured with an selective ion electrode. The adsorption of fluoride ions on $AgNP_{(Xs)}$ was initially shown by finding a decrease in the absorbance reading of $AgNP_{(Xs)}$ at λ=427 and later the results were confirmed by measuring the fluoride ions using an ion selective electrode. The maximum complexation of the fluoride ions with $AgNP_{(Xs)}$ was 53%. The efficiency of the treatment decreased when the fluoride concentration increased above 1.5 µg mL^{-1}. These findings will help to lay a foundation for the development of clean methods of fluoride removal from water using nanotechnology

Keywords: Fluoride removal; Green synthesis; Silver nanoparticles; *Xanthium stumarium*.

INTRODUCTION

Fluorinated compounds are widely used in industry for different purposes. Fluorinated compounds are used in aluminium production and released in the production of tiles, ceramics, and bricks in kilns. Phosphate fertilizers contain an average of 3.8% fluorine. Municipal water fluoridation also uses fluorosilicic acid, sodium fluoride, and sodium hexafluorosilicate.[1-2] Fluoride can toxic to both plants and animals and may occur with contamination from airborne fluoride or the presence of high levels of fluoride in ground water. Sea water contains approximately 1.3 mgL^{-1} of fluoride. The ground water in areas containing fluoride-enriched minerals may contain up to 10 to 2800 mgL^{-1} of fluoride.[3] Industrial discharges can contribute to the fluoride pollution of rivers.[4] In China, the ground waters of some villages were contaminated by more than 8 mgL^{-1}fluoride.[5] In Canada, fluoride levels have been reported for municipal drinking water of <0.05–0.2 mgL^{-1} (non-fluoridated) and 0.6–1.1 mgL^{-1} (fluoridated), and for well water of 3.3 mgL^{-1}. Approximately 0.2% of the population in USA is exposed to more than 2.0 mgL^{-1} of fluoride in drinking water.[3] In the Netherlands, the average fluoride content of drinking water was found below 0.2 mgL^{-1} for the whole year.[5] The fluoride content in drinking water in some African countries could be high due to the presence of

---

[a]Department of Agricultural Chemistry, The University of Agriculture Peshawar, Pakistan; [b]Department of Soil and Environmental Sciences, The University of Agriculture Peshawar, Pakistan; [c]Pakistan Institute of Nuclear Science and Technology, Nilor Islamabad, Pakistan; [d]Department of Food Science and Technology, The University of Agriculture Peshawar, Pakistan. For correspondence: Mudassar Iqbal, Department of Agricultural Chemistry, The University of Agriculture Peshawar, Pakistan; E-mail: mudassariqbal@aup.edu.pk

fluoride-enriched minerals in soil.[3] In Central Australia, a survey of groundwater boreholes revealed that half of the water samples contained fluoride levels above 1.5 mgL^{-1}, with a range of 3–9 mgL^{-1}.[6]

Several laboratory based fluoride toxicity studies have been carried out on different animals. When fluoride was given to rats orally for 3–5 weeks, in drinking water with 16 $mgL^{-1}$of fluoride, there was inhibition of bone mineralization, delayed healing of bone fractures, and a marked reduction in collagen synthesis. A more severe effect with bone fragility was observed with fluoride concentrations exceeding 64 mgL^{-1}. Mice, that were administered fluoride in drinking water, were found with defective bone structural remodeling, nephrosis, mineralization of the myocardium, hepatic megalocytosis, and seminiferous tubules degeneration.[2] An *in vitro* study of mammalian cells revealed genetic damage that ultimately indirectly affected the synthesis of the protein responsible for DNA synthesis.[2,7]

Nanotechnology is gaining much attention with the development of various products for the removal of pollutants from the environment. Particles of 1–100 nm size, in at least one dimension, are considered to be nanoparticles.[8] With the decrease in the particle size, the surface area to volume ratio of nanoparticles increases which leads to improved physical, chemical, and biological properties.[9] Nanoparticles can be produced by various approaches including chemical,[10] electrochemical,[11] physical,[12] and biological techniques.[13] The majority of the chemical procedures used for the fabrication of nanoparticles are not eco-friendly as they involve the use of toxic and hazardous chemicals that can cause biological risk. Similarly, most of physical methods involve the use of high energy which are not cost effective. These limitations have led to the development of eco-friendly methods for the synthesis of nanoparticles. Hence, the production of nanoparticles using plant extracts is gaining more attention. Plant-mediated green synthesis of silver nanoparticles has been reported for various useful activities including biomedical, antifungal, antimicrobial, and antiviral activities, etc.[14-15] The biomolecules present in plant extracts, including flavonoids, polyphenols, dehydrogenases, reductases, and a few organic acids play a vital role in the bio-reduction of metal ions to nanoparticles.[16]

Developing a green technology for the treatment of fluoride-contaminated water may be of value for use in agriculture as well as in providing safe drinking water for domestic use. In this work we investigated the green synthesis of stable silver nanoparticles ($AgNP_{(Xs)}$) using an aqueous concentrate of *Xanthium stumarium* and evaluated their efficacy for the removal of fluoride from water sample. To the best of our knowledge this is the first study that reports on fluoride removal from water using green synthesized $AgNP_{(Xs)}$.

METHODOLOGY

All the chemicals and reagents used in this study were of analytical grade. Freshly prepared distilled water was used for the extractions and deionized water was used for all other activities.

Preparation of the plant extract: Fresh leaves of *Xanthium stumarium* were collected from district Kohat, Khyber Pakhtunkhwa, Pakistan, and washed with clean water followed by distilled water to remove debris and dirt particles. The plant material was air dried for 14 days at room temperature to prevent the destruction of thermo-labile biomolecules. After drying, the sample was milled to a coarse powder and a 20 g powdered sample was added to 200 mL of double distilled water and heated at 60ºC for 30 min. The aqueous extract was filtered using muslin cloth followed by filter paper (Whatman no. 1). The filtrate was stored at 4ºC for further use.

Qualitative phytochemical analysis: The qualitative analysis of phytochemicals such as reducing sugars, alkaloids, tannins, alkaloids, anthoquinones, steroids, phenols, terpeniods, and flavonoids was carried out according to the methods of Trease and Evans.[17]

Biosynthesis of silver nanoparticles: The silver nanoparticles ($AgNP_{(Xs)}$) were synthesized by reacting aqueous metal salts ($AgNO_3$ 1 mM solution) with the aqueous filtrate of *Xanthium stumarium*.[15,18] For this purpose both reactants were mixed in a 1:1 (v/v) ratio at 30ºC for 12 hours under continuous stirring, which yielded a dark brown reaction solution.

Characterization of synthesized silver nanoparticles

SURFACE PLASMON RESONANCE SPECTROSCOPY (UV-VIS): The change in the color from brown to dark brown after incubation was the preliminary indicator of the synthesis of $AgNP_{(Xs)}$. The synthesis of $AgNP_{(Xs)}$ was confirmed by analyzing their kinetic behavior using a UV-visible spectrophotometer (Optima SP3000+, Japan). The synthesized $AgNP_{(Xs)}$ were scanned between 350–700 nm with sampling intervals of 1 nm. Diluted aliquots of aqueous *Xanthium stumarium* filtrate were used as a blank.

FOURIER TRANSFORMS INFRARED (FTIR) SPECTROSCOPY: FTIR analysis of the synthesized nanoparticles was used to assess the types of functional groups present in the biomolecules responsible for reduction as well as capping material. FTIR was performed on a Prestige-21 spectrophotometer; (Shimadzu, Japan) using a 450–4,000 cm^{-1} scanning range at a resolution of 4 cm^{-1} using the potassium bromide (KBr) pellet method.

SCANNING ELECTRON MICROSCOPY (SEM) ANALYSIS: The morphology of the synthesized nanoparticles was studied using a scanning electron microscope (JEOL JSM 5910 SEM instrument) at 20 kV. The $AgNP_{(Xs)}$ sample was extracted through centrifugation (10,000 resolution min^{-1} for 15 min) to obtain suspended particles. The particles were re-suspended in 1 mL distilled water and subjected to sonication for 30 min. From this, one drop of sample was placed on a 1 cm^2 glass slide, dried under UV-lamp, and sputter coated on gold grids before the SEM examination under different magnifications.

Defluoridation studies of simulated fluoride-contaminated water sample: The adsorption process of fluoride by $AgNP_{(Xs)}$, in simulated fluoride-contaminated water, was studied in the laboratory by indirect fluoride determination. The decreasing in the intensity of the SPR peak suggested a directly proportional decrease in the concentration of $AgNP_{(Xs)}$, and hence an inversely proportional complexion and/or adsorption of fluoride ions by $AgNP_{(Xs)}$. For this purpose different concentrations of working and standard solutions of fluoride ions were prepared by serial dilution (0.25, 0.5, 1.0, 1.5, 1.75, 2.5, and 5.0 µg mL^{-1}) using 5.0 µg mL^{-1} stock solution, prepared using pure sodium fluoride (NaF, Sigma) salt in deionized distilled water.

Both aqueous $AgNP_{(Xs)}$ and fluoride solutions were mixed together in a 1:1 (v/v) ratio at 30ºC and allowed to stand for 4 hours before being analyzed using UV-Vis spectroscopy for their SPR region change. Similarly, the absorbance value was also measured at a fixed wavelength (427 nm) to indicate increases or decreases in the complexion and/or adsorption of fluoride on the surface of the $AgNP_{(Xs)}$.

Fluoride determination: After the simulated fluoride-contaminated water samples were treated with $AgNP_{(Xs)}$ they were centrifuged at 10,000 resolution min^{-1} for 15 minutes, the supernatant solution was separated, and the fluoride ion concentration was measured using a F-sensitive electrode (ISE F 800 DIN, WTW Wilhelm, Germany) coupled to an ion meter (Inolab pH/Ion 735 WTW Wilhelm, Germany) by following the modified procedure explained elsewhere[19] using TISAB II buffer.[20] A fluoride standard curve was made using a series of seven standards (0.25, 0.5, 1.0, 1.5, 1.75, 2.5, and 5.0 $\mu g\ mL^{-1}$) by diluting NaF in distilled water.

Data analysis: The data was analyzed using software OriginPro 8®. The fluoride content in the samples was calculated through logarithmic regression using Microsoft Excel. The results are presented as a mean of the replicated data.

RESULTS

Phytochemical composition: Qualitative analysis of aqueous leaf extract of *Xanthium stumarium* confirmed the presence of biomolecules such as reducing sugars, tannins, alkaloids, phenols, terpeniods, and flavonoids, while steroids and anthraquinones were not detected (Table).

Table. Phytochemical constituents of the *Xanthium stumarium* aqueous extract

Phytochemical	Presence of phytochemical*
Reducing sugars	+
Tannins	+
Alkaloids	+
Phenols	+
Terpeniods	+
Flavonoids	+
Steroids	–
Anthraquinones	–

* + = phytochemical present, – = phytochemical absent.

It is a well established fact that some of the secondary metabolites present in biological extracts act as both reducing and capping agents. Some of the identified phytochemicals will be responsible for the reduction of Ag^+ to Ag^0 and later on will also act as a stabilizing agent to avoid the agglomeration of $AgNP_{(Xs)}$.

Synthesis of silver nanoparticles (AgNP$_{(Xs)}$): The aqueous extract of *Xanthium stumarium* upon treatment with 1 mM aqueous $AgNO_3$ solution at 30ºC caused a visible change in the colour of reaction solution to dark brown and its intensity increased as the time increased. This was a clear indication of the formation of silver nanoparticles in the reaction. The presence of biomolecules such as tannins and polyphenols, etc., causes the reduction of Ag^+ to intermediate complexes with the phenolic OH group of hydrolysable biomolecules in the plant extracts. These intermediate complexes then undergo oxidation with the consequent reduction of Ag^+ to AgNP$_{(Xs)}$.[20]

Characterization of silver nanoparticles:

ULTRAVIOLET-VISIBLE (UV-VIS) SPECTROSCOPY ANALYSIS: The persistent dark brown colour of synthesized AgNP$_{(Xs)}$ is due to a specific surface plasmon resonance (SPR) region. The size of the AgNP$_{(Xs)}$ plays an important role towards a blue or red shift of the SPR peak. Smaller size AgNP$_{(Xs)}$ tend to fall in the blue shift region (around 400 nm) while large sized AgNP$_{(Xs)}$ increase the SPR wavelength towards the red shift region.[21] In this study, the UV-visible spectra of AgNP$_{(Xs)}$ synthesized by using an aqueous extract of *Xanthium stumarium* showed a strong SPR peak at λ_{max} = 427 nm (Figure 1). These results agree with previous work on the green synthesis of AgNP$_{(Xs)}$ where the wavelength range was 400–500 nm.[21-23]

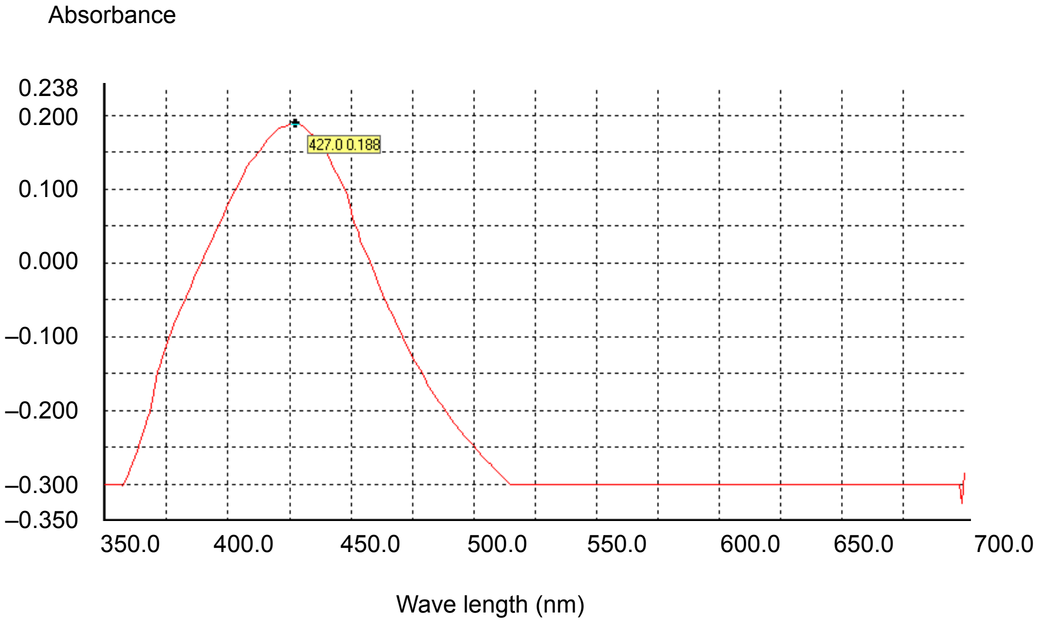

Figure 1. UV-Vis spectrum of AgNP$_{(Xs)}$ obtained from bio-reduction and stabilizing by an aqueous extract of *Xanthium stumarium*.

SCANNING ELECTRON MICROSCOPY (SEM) ANALYSIS: To avoid the imaging of any residues, as well as non-reactive biomolecules, present in the aqueous extract of *Xanthium stumarium,* the AgNP$_{(Xs)}$ were washed with ethanol and then centrifuged at 10,000 revolutions/min for 15 min. The supernatant was then discarded and the solid material was used for SEM imaging. The image showed that the average size for the $AgNP_{(Xs)}$ was 28 nm and they appeared as relatively uniform nano rods (Figure 2). The SEM image did not show any agglomerated particles.

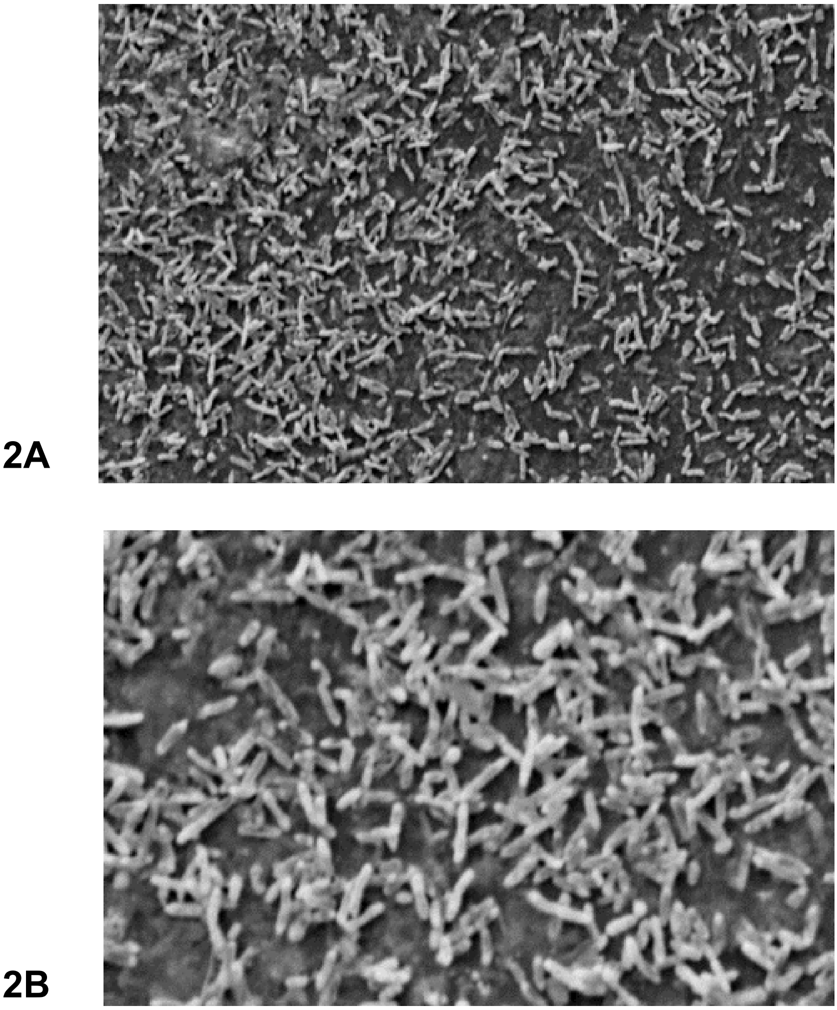

Figures 2A and 2B. Scanning Electron Microscopy images of $AgNP_{(Xs)}$ synthesized using an aqueous extract of *Xanthium stumarium*.

FOURIER TRANSFORMS INFRARED SPECTROSCOPY (FTIR) ANALYSIS: The functional group composition of the bio-synthesized $AgNP_{(Xs)}$ was assessed using FTIR analysis. The entire observed spectrum was measured in the range of 500–4000 cm^{-1} at a resolution of 4 cm^{-1}(Figure 3). The IR bands observed at 3448 cm^{-1}correspond to O-H stretch and can be assigned to hydroxyl groups. The band at 2893 cm^{-1} is of alkane C-H, the peak stretching on 2075 cm^{-1} corresponds to alkyne stretch, and the weak band at 1427 cm^{-1} is generally related to the C-C stretch of the aromatic ring. All the IR banks present in the spectral analysis of the $AgNP_{(Xs)}$ indicate the existence of very important functional groups of phytochemicals such as flavonoids, phenols, amino acids, etc., which play an important role in the fabrication of metal nanoparticles by reducing metal ions and preventing agglomeration, thereby stabilizing the $AgNP_{(Xs)}$.

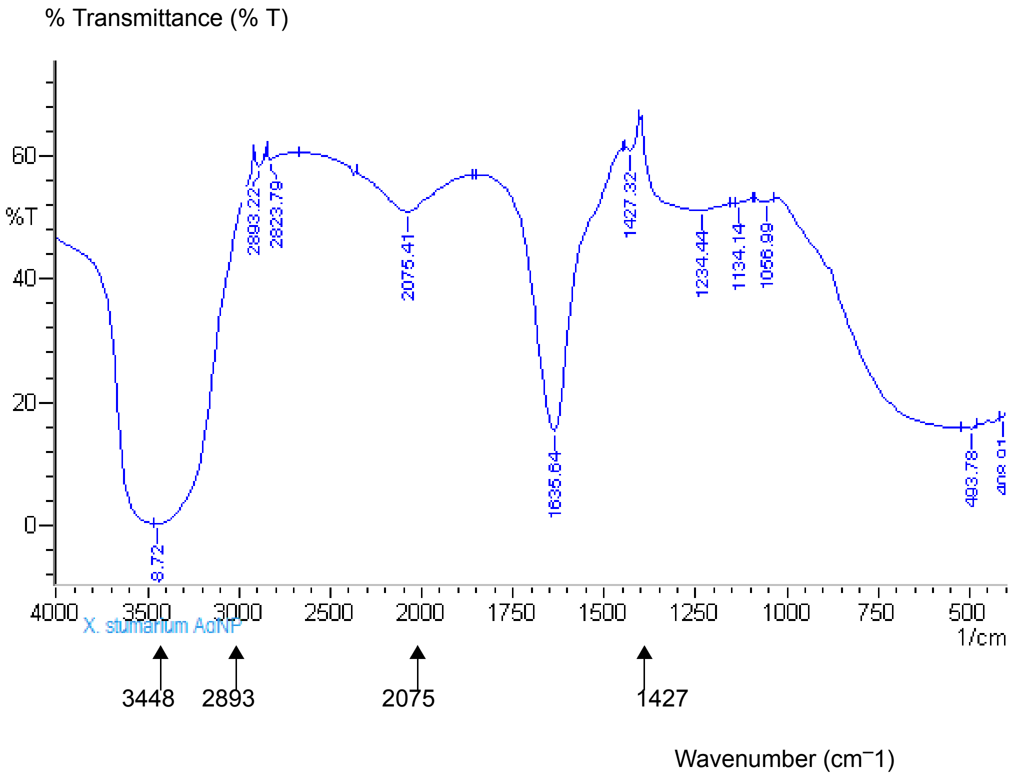

Figure 3. FT-IR spectrum of silver nanoparticles bio-synthesized through an aqueous extract of *Xanthium stumarium.*

Defluoridation studies of the simulated fluoride-contaminated water samples: The $AgNP_{(Xs)}$ upon treatment with fluoride solution were tested for their SPR absorbance shift at λ=427 nm (absorbance maxima of $AgNP_{(Xs)}$). The trend line depicted in Figure 4 confirmed the maximum adsorption of fluoride on $AgNP_{(Xs)}$while using 1.5 µg mL^{-1} fluoride solution.

Similarly 0.5 and 1.0 µg mL^{-1} fluoride solutions also showed complexation with $AgNP_{(Xs)}$ with a decreasing trend line with respect to an increasing concentration. With a test concentration above 1.5 µg mL^{-1} less complexation was evident from the absorbance reading. The decrease in the absorbance with more complexation of F ions through UV-Vis spectroscopy was confirmed by measuring the fluoride ion concentration of the $AgNP_{(Xs)}$-treated water samples through the conventional fluoride determination procedure using an ion selective electrode.

Fluoride determination: The standard curve for the determination of the fluoride content in the water samples was built by plotting the electric potential (mV) vs log of a standard fluoride concentration (µg mL^{-1}). The linear calibration curve gave the following equation.

$$Y = -56.415x + 86.083 \qquad (R^2 = 0.9967)$$

A clear linear relationship between E (mV) verses log fluoride ion concentration (μg mL^{-1}) was observed with the R^2 calculated as 0.9967. The slope measurement of –56.415 mV was close to the theoretical value of –59.2 mV at 25ºC. The difference observed between the theoretical and calculated values could be due to a temperature effect.

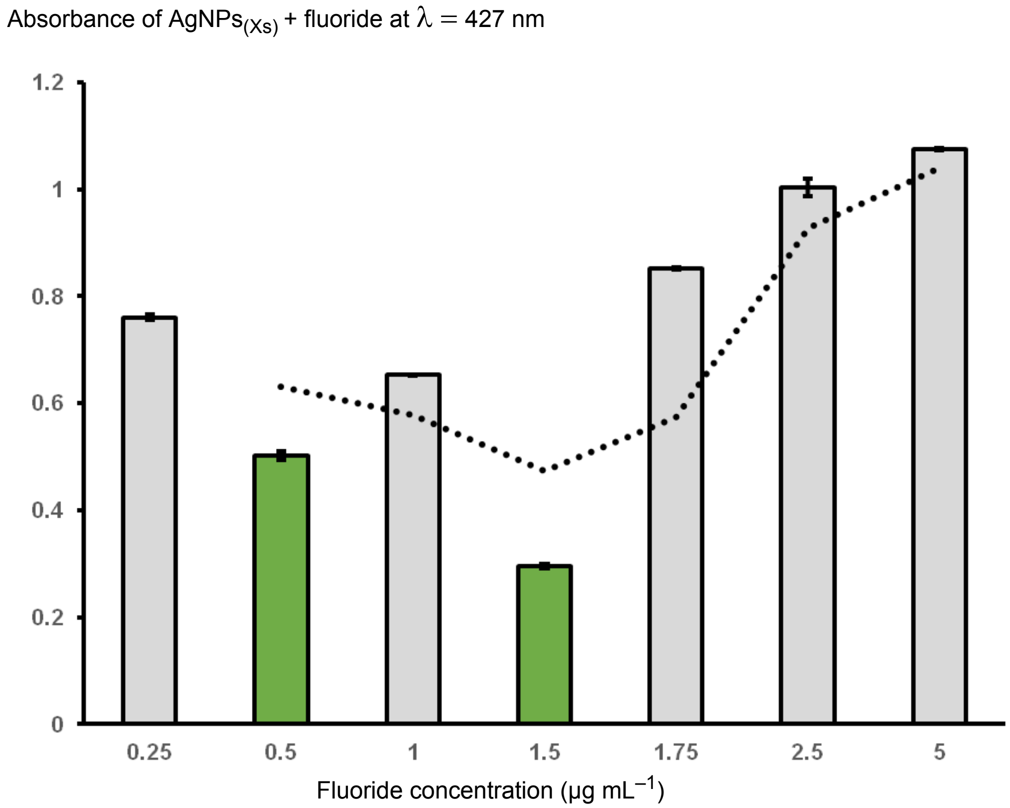

Figure 4. Absorbance of $AgNPs_{(Xs)}$ + fluoride at λ = 427 nm for various concentrations of fluoride.

Determination of fluoride in water after treatment with $AgNP_{(Xs)}$: The total fluoride content in the post $AgNP_{(Xs)}$ treated fluoride-contaminated water samples was measured using an ion selective electrode. Figure 5 clearly shows that at lower concentrations up to 1.5 μg mL^{-1} the fluoride absorption was high while with the increased fluoride concentrations the complexation of fluoride with $AgNP_{(Xs)}$ decreased. The maximum adsorption of fluoride ions (0.8 μg mL^{-1}, 53%) was observed when 1.5 μg mL^{-1} fluoride solution (1:1, v/v) was treated with $AgNP_{(Xs)}$ solution (Figure 6). Interestingly, it was found that higher concentrations of fluoride ions did not cause a greater complexation with $AgNP_{(Xs)}$. This may be due to a lesser availability of reactive sites on to the surface of the $AgNP_{(Xs)}$.

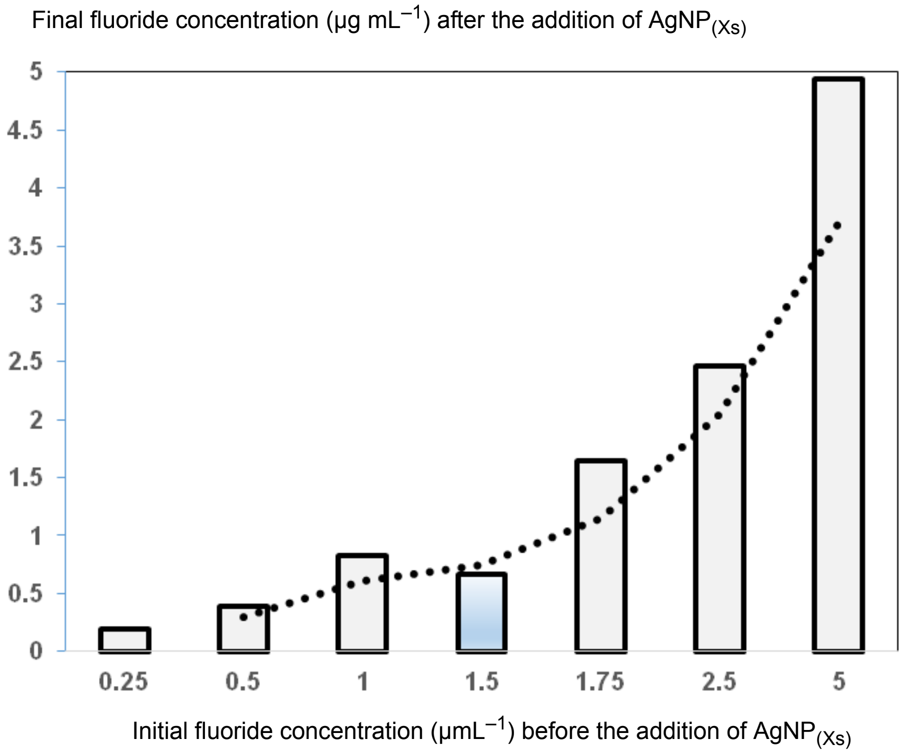

Figure 5. Effect of AgNP$_{(Xs)}$ on the final concentration of fluoride in water samples with various initial fluoride concentrations (μmL^{-1}).

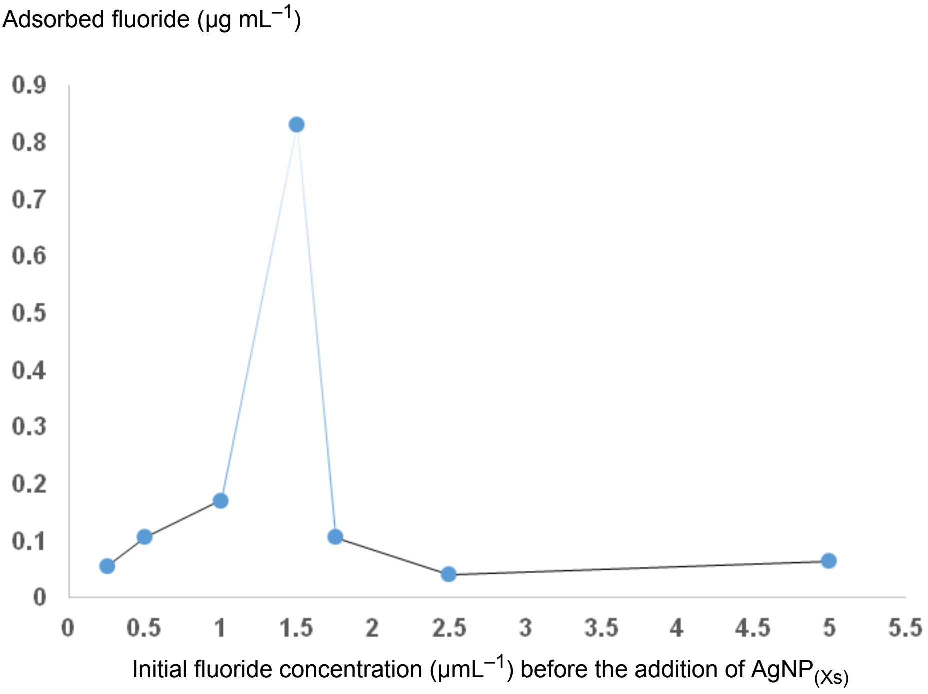

Figure 6. Concentration of fluoride ions (μmL^{-1}) adsorbed on to AgNP$_{(Xs)}$ for various initial fluoride concentrations (μmL^{-1}).

DISCUSSION

Nanotechnology is an emerging field of science and is transforming applied sciences to the next level. Water pollution caused by various biological and chemical contaminants is posing a serious problem to health and the use of nanotechnology for the treatment of contaminated water would be a way forward. The green synthesis of nanomaterial is gaining much attention due to its nontoxic and eco-friendly nature. In this project, the synthesis of $\mathrm{AgNP}_{(\mathrm{Xs})}$ using an aqueous extract of *Xanthium stumarium* was achieved at room temperature. Other scientists have also reported the use of various plant extracts for the fabrication of silver nanoparticles.[18,24-26] These particles possess a tremendous biological potential when tested against various pathogens.[27,28] Nanosized metal oxides have also been reported for the successful removal of heavy metals from wastewater.[29] The use of bimetallic Cu-Ag nanoparticles (Np) has been reported for the treatment of various organic and inorganic contaminants of waste water.[30] Fluoride contamination in drinking water can lead to various serious effects, especially on skeletal tissues. Skeletal fluorosis, with adverse changes in bone shape and structure, may occur with a drinking water fluoride concentration of 3–6 mg/L and the use of drinking water with a fluoride concentration greater than 10 mg/L may be associated with the more serious condition of crippling skeletal fluorosis.[31] Acute fluorosis caused by excessive fluoride contamination in groundwater is also a serious issue in more than 20 developed and developing countries.[32] If an alternative safe water source can not be found, the removal of fluoride from contaminated drinking water is the only solution to this problem. Over the past few years, extensive research has been carried regarding the defluoridation of both drinking and waste water, using the principles of adsorption,[33] ion exchange,[34] electrodialysis,[35] etc. Another cost efficient technology for the removal of fluoride from water is based on the use of nanomaterials. Many researchers have reported the successful adsorption of fluoride using various metal oxides and hydroxide nanoparticles.[36] The fluoride adsorption depends on the diffusion of fluoride ions to the external adsorbent layer. The fluoride ions then travel to the particle surface and, finally, the adsorbed fluoride ions are transferred via intra particle diffusion to the internal porous material.[37]

CONCLUSION

In conclusion, the successful and rapid synthesis of $\mathrm{AgNP}_{(\mathrm{xs})}$, with an average size 28 nm, was achieved using an aqueous extract of *Xanthium stumarium*. Later these $\mathrm{AgNP}_{(\mathrm{Xs})}$ were used for the successful complexation of fluoride ions in drinking water. They were able to bind fluoride at a concentration of up to 1.5 $\mu\mathrm{g\ mL}^{-1}$ We opined that the $\mathrm{AgNP}_{(\mathrm{Xs})}$ synthesized using above protocol could generate materials in a sufficient quantity for them to be used in the defluoridation of drinking water.

ACKNOWLEDGMENT

We are thankful to The University of Agriculture, Peshawar, Pakistan, for providing us working space to complete this research.

REFERENCES

1 World Health Organization International Agency for Research on Cancer (IARC) Working Group on the Evaluation of the Carcinogenic Risk of Chemicals on Humans. Some aromatic amines, anthraquinones and nitroso compounds, and inorganic fluorides used in drinking-

water and dental preparations. IARC Monographs on the evaluation of the carcinogenic risk of chemicals to humans. Vol. 27. [Views and expert opinions of a working group on the evaluation of the carcinogenic risk of chemicals on humans which met in Lyon, France. 1981 Feb 10-17. Geneva: WHO International Agency for Research on Cancer; 1982. pp. 237-303.

2 WHO. Guidelines for drinking-water quality. 3rd ed. Vol 1, Recommendations. Geneva: World Health Organization (WHO); 2004.

3 US EPA. Drinking water criteria document on fluoride (TR-823-5). Washington, DC: US Environmental Protection Agency, Office of Drinking Water; 1985.

4 Slooff W, Eerens HC, Janus JA, Ros JPM, Janssen PJCM, Knaap AGAC, et al. Basisdocument fluoriden. (Report No. 758474005). Bilthoven, Netherlands: National Institute of Public Health and Environmental Protection;1988. [in Dutch].

5 Fuhong R, Shuqin J. Distribution and formation of high-fluorine groundwater in China. Environmental Geology and Water Sciences 1988;12:3-10.

6 Fitzgerald J, Cunliffe D, Rainow S, Dodds S, Hostetler S, Jacobson G. Groundwater quality and environmental health implications: Anangu Pitjantjatjara Lands South Australia. Canberra, Australia: Bureau of Rural Sciences; 2000. pp. 56.

7 Slooff W, Eerens HC, Janus JA, Ros JPM. Integrated criteria document fluorides: effects (Report No. 758474010). [This document is the English edition of the Basisdocument Fluoriden, Report No. 758474005, 1988 Nov, reference number 4 on this page]. Bilthoven, The Netherlands: National Institute of Public Health and Environmental Protection; 1989. Available from: https://www.researchgate.net/publication/263715796_Integrated_criteria_document_Fluorides/link/00b4953bbea8f375ee000000/download

8 Wadekar PP, Patil JA. A review on gold nanoparticles synthesis and characterization [review]. Universal Journal of Pharmaceutical Research 2017;2(4):65-9. Available from: http://ujpr.org

9 Yusuf FS, Yunus AA, John DF, Chigbo UJ. Abacavir loaded nanoparticles: preparation, physicochemical characterization and *in vitro* evaluation. Universal Journal of Pharmaceutical Research.2016;1(2):19-24. Available from: http://ujpr.org

10 Hyeon T. Chemical synthesis of magnetic nanoparticles. Chem Commun (Camb) 2003;8:927-34.

11 Yin B, Ma H, Wang S, Chen S. Electrochemical synthesis of silver nanoparticles under protection of poly (N-vinylpyrrolidone). The Journal of Physical Chemistry B 2003;107:8898-904.

12 Eliaz ES, Grossman E, Fisher D, Gouzman I, Henis Z, Pecker S, et al. Synthesis of nanoparticles with femtosecond laser pulses. Physical Review B 2004;69:144119.

13 Thakkar KN, Mhatre SS, Parikh RY. Biological synthesis of metallic nanoparticles. Nanomedicine: Nanotechnology, Biology and Medicine 2010;6:257-62.

14 Mallikarjuna K, Narasimha G, Dillip GR, Praveen B, Shreedhar B, Sree Lakshmi C, et al. Green synthesis of silver nanoparticles using *Ocimum* leaf extract and their characterization. Digest Journal of Nanomaterials and Biostructures 2011;6:181-6.

15 Li S, Shen Y, Xie A, Yu X, Qiu L, Zhang L, Zhang Q. Green synthesis of silver nanoparticles using *Capsicum annuum* L. extract. Green Chemistry 2007;9:852-8.

16 Iravani S. Green synthesis of metal nanoparticles using plants. Green Chemistry 2011;13:2638-50.

17 Trease GE, Evans WC. Phytochemical screening. In: Trease GE, Evans WC. A textbook of pharmacognosy. 13th ed. London: Bailliere Tinall Limited; 1989. pp. 541.

18 Abdelmoteleb A, Valdez-Salas B, Carrillo-Beltran M, Hernandez DD, Gonzalez-Mendoza D. Green synthesis of silver nanoparticles using *Pluchea sericea* a native plants from Baja California, Mexico and their potential application as antimicrobials. Iran J Sci Technol A 2018;42:457-63. doi:10.1007/s40995-016-0019-6.

19 Amanlou M, Hosseinpour M, Azizian H, Khoshayand MR, Navabpoor M, Souri E. Determination of fluoride in the bottled drinking waters in Iran. Iran J Pharm Res 2010;9:37-42.

20Bulut E, Özacar M. Rapid, facile synthesis of silver nanostructure using hydrolyzable tannin. Industrial & Engineering Chemistry Research 2009;48:5686-90. doi:10.1021/ie801779f.

21 Sönnichsen C, Reinhard BM, Liphardt J, Alivisatos AP. A molecular ruler based on plasmon coupling of single gold and silver nanoparticles. Nat Biotechnol 2005;23:741-5. doi:10.1038/nbt1100https://www.nature.com/articles/nbt1100#supplementary-information.

22 Edison TJI, Sethuraman MG. Instant green synthesis of silver nanoparticles using *Terminalia chebula* fruit extract and evaluation of their catalytic activity on reduction of methylene blue. Process Biochemistry 2012;47:1351-7. doi:https://doi.org/10.1016/j.procbio.2012.04.025.

23 Park J, Choi JS. Capacitance-voltage characteristics of MIS capacitors using polymeric insulators. Journal of Information Display 2008;9:1-4. doi:10.1080/15980316.2008.9652049.

24 Hussain M, Raja NI, Mashwani Z-U-R, Naz F, Iqbal M, Aslam S. Green synthesis and characterisation of silver nanoparticles and their effects on antimicrobial efficacy and biochemical profiling in *Citrus reticulata.* IET Nanobiotechnol 2018;12(4):514-9. doi:10.1049/iet-nbt.2017.0153.

25 Joshi N, Jain N, Pathak A, Singh J, Prasad R, Upadhyaya CP. Biosynthesis of silver nanoparticles using *Carissa carandas* berries and its potential antibacterial activities. J Sol-Gel Sci Techn 2018;86:682-9. doi:10.1007/s10971-018-4666-2.

26 Manju AS, Vivek PB. Plant mediated green synthesis of silver nanoparticles using seed extract of *Psoralea corylifolia* and to study its characterization and antimicrobial activity. Res J Biotechnol 2018;13:52-9.

27 Ahmadi O, Jafarizadeh-Malmiri H, Jodeiri N. Eco-friendly microwave-enhanced green synthesis of silver nanoparticles using *Aloe vera* leaf extract and their physico-chemical and antibacterial studies. Green Process Synth 2018;7:231-40. doi:10.1515/gps-2017-0039.

28 Jung J, Kasi G, Seo J. Development of functional antimicrobial papers using chitosan/starch-silver nanoparticles. Int J Biol Macromol 2018;112:530-6. doi:10.1016/j.ijbiomac.2018.01.155.

29 Hua M, Zhang S, Pan B, Zhang W, Lv L, Zhang Q. Heavy metal removal from water/wastewater by nanosized metal oxides: A review. J Hazard Mater 2012;211-212:317-31. doi:https://doi.org/10.1016/j.jhazmat.2011.10.016.

30 Ismail M, Khan MI, Khan SB, Khan MA, Akhtar K, Asiri AM. Green synthesis of plant supported Cu-Ag and Cu-Ni bimetallic nanoparticles in the reduction of nitrophenols and organic dyes for water treatment. J Mol Liq 2018;260:78-91. doi:10.1016/j.molliq.2018.03.058.

31 IPCS. Fluorine and fluorides. Environmental Health Criteria 36. Geneva: World Health Organization, International Programme on Chemical Safety; 1984.

32 Meenakshi, Maheshwari RC. Fluoride in drinking water and its removal. J Hazard Mater 2006;137:456-63. doi:https://doi.org/10.1016/j.jhazmat.2006.02.024.

33 Raichur A, Basu MJ. Adsorption of fluoride onto mixed rare earth oxides. Sep Purif Technol 2001;24:121-7.

34 Singh G, Kumar B, Sen P, Majumdar J. Removal of fluoride from spent pot liner leachate using ion exchange. Water Environment Research 1999;71:36-42.

35 Hichour M, Persin F, Sandeaux J, Gavach C. Fluoride removal from waters by Donnan dialysis. Sep Purif Technol 1999;18:1-11.

36 Bhattacharya S. Application of nanostructured materials in fluoride removal from contaminated groundwater. European Water 2017;58:87-93.

37 Mohapatra M, Anand S, Mishra BK, Giles DE, Singh P. Review of fluoride removal from drinking water. J Environ Manage 2009;91:67-77.